STRUCTURAL SCIENCE
CRYSTAL ENGINEERING
MATERIALS

Volume 73 (2017)

Supporting information for article:

X-ray, dielectric, piezoelectric and optical analysis of a new NLO 8-hydroxyquinolinium hydrogen squarate crystal

Sahil Goel, Harsh Yadav, Nidhi Sinha, Budhendra Singh, Igor Bdikin and Binay Kumar

S1. Formation of α-chain by hydrogen squarate mono-anions

In present HQS crystal structure, hydrogen squarate mono-anion displays a α-chain supramolecular pattern (Fig. S1). In α-chain, the ⁻O–C=C–OH α-diketone enolate group (⁻O5–C14=C13–O4–H4A) is involved in short O4–H4A···O5 hydrogen bonds with two neighbouring hydrogen squarate mono-anions. The other two O atoms (O3 & O2) are saturated by hydrogen bond donors [protonated 8-hydroxyquinolinium cation] through C2–H2···O3 and N1–H1···O2 hydrogen bonds (Fig. S1). This assembly of 8-hydroxyquinolinium cations and hydrogen squarate mono-anions leads to infinite supramolecular chain running along '*a*' crystallographic axis.

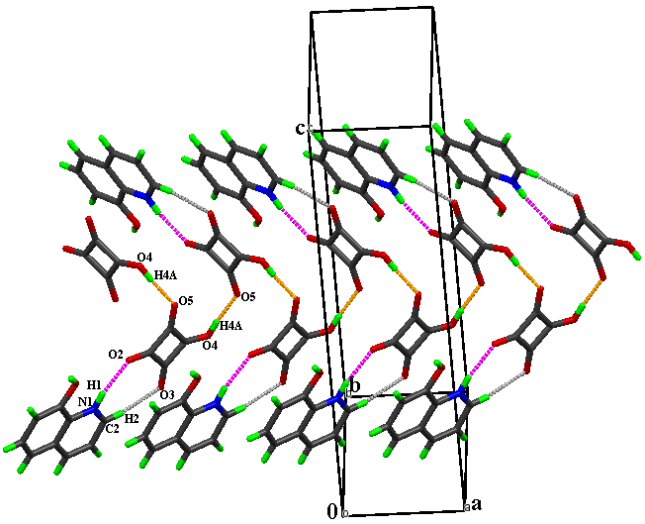

Figure S1 α-chain of hydrogen squarate mono-anions surrounded by hydrogen bonded 8-hydroxyquinolinium cations.

S2. Comparison of two unit cells

The molecular packing diagrams of bis(8-hydroxyquinolinium) squarate (Monoclinic; $P2_1/c$) and 8-hydroxyquinolinium hydrogen squarate crystal (Orthorhombic; $P2_12_12_1$) were compared using CrystalCMP software and their comparison is shown in Fig. S2 (Rohlíček *et al.*, 2016). In Fig. S2, bis(8-hydroxyquinolinium) squarate and 8-hydroxyquinolinium hydrogen squarate unit cell packing diagrams are depicted in red and yellow color, respectively.

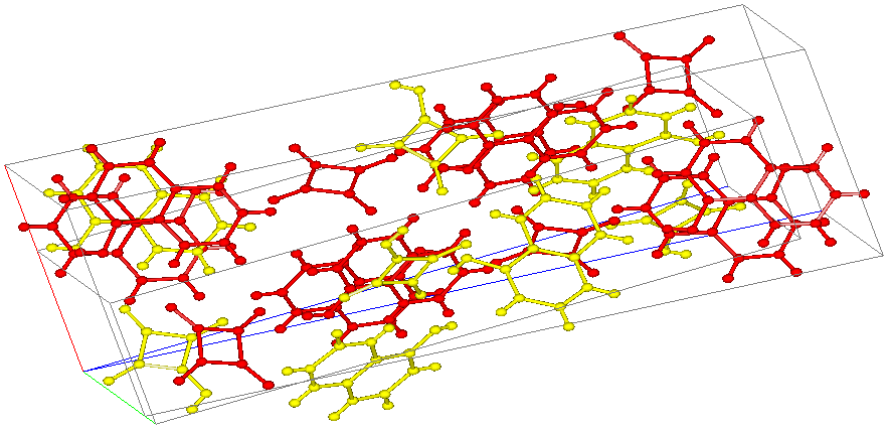

Figure S2 Red-yellow pair views to see the difference between the crystal packing of bis(8-hydroxyquinolinium) squarate (shown in red) and 8-hydroxyquinolinium hydrogen squarate (shown in yellow).

S3. Crystallographic data

The isotropic displacement parameters and final refined fractional atomic positions for the titled compound are given in Table S1, and the anisotropic displacement parameters of non hydrogen atoms are given in Table S2. Table S3 summarizes the H-atom coordinates and isotropic displacement parameters. Table S4 lists the values of torsion angles for the titled molecule.

Table S1 Fractional atomic coordinates ($\times 10^4$) and equivalent isotropic displacement parameters ($Å^2 \times 10^3$) for 8-hydroxyquinolinium hydrogen squarate. U_{eq} is defined as 1/3 of the trace of the orthogonalised U_{IJ} tensor.

Atom	***X***	***y***	***z***	**U(eq)**
O2	-8725(4)	-9579(3)	-579.4(10)	41.9(7)
O5	-12637(4)	-11581(3)	175(1)	41.2(7)
O4	-15004(5)	-12779(4)	-1028.1(10)	47.6(8)
O3	-10964(5)	-11035(3)	-1768.1(10)	45.5(7)
N1	-5613(5)	-8385(3)	-1438.8(12)	34.4(7)
C9	-3675(6)	-7418(4)	-1384.3(14)	30.5(8)
O1	-4491(5)	-7200(4)	-386.5(11)	53.0(8)
C8	-3083(7)	-6774(4)	-840.0(15)	35.2(9)
C14	-12149(6)	-11375(4)	-353.6(15)	31.9(8)
C10	-2332(6)	-7066(4)	-1889.3(14)	31.0(8)
C7	-1167(7)	-5790(5)	-806.9(16)	43(1)

C2	-6321(7)	-8968(5)	-1941.8(16)	40.1(9)
C12	-11411(6)	-11142(4)	-1242.5(15)	32.7(8)
C4	-3094(7)	-7709(4)	-2423.2(15)	39.8(9)
C11	-10364(6)	-10510(4)	-693.3(14)	31.6(8)
C13	-13175(6)	-11911(4)	-886.6(15)	32.9(8)
C5	-366(7)	-6060(4)	-1835.9(16)	40.3(9)
C3	-5073(8)	-8624(4)	-2451.0(17)	42.4(10)
C6	167(7)	-5441(5)	-1305.1(16)	43.3(10)

Table S2 Anisotropic displacement parameters ($Å^2 \times 10^3$) for 8-hydroxyquinolinium hydrogen squarate. The anisotropic displacement factor exponent takes the form: $-2\pi^2[h^2a^{*2}U_{11}+2hka^*b^*U_{12}+\ldots]$.

Atom	U_{11}	U_{22}	U_{33}	U_{23}	U_{13}	U_{12}
O2	47.1(15)	48.7(16)	29.8(13)	-6.5(12)	2.4(13)	-10.7(14)
O5	36.6(14)	65.8(19)	21.2(13)	4.0(11)	1.9(12)	2.4(13)
O4	43.7(15)	72(2)	27.0(13)	-5.5(14)	4.0(12)	-18.6(15)
O3	49.8(16)	64.2(19)	22.3(13)	-0.6(13)	5.8(12)	-10.8(15)
N1	36.1(17)	38.5(18)	28.6(16)	-0.9(13)	1.9(14)	-2.5(15)
C9	33.6(18)	30.2(19)	27.8(18)	0.0(15)	-3.0(16)	0.8(16)
O1	63.4(19)	67(2)	28.5(14)	-8.5(14)	8.0(14)	-16.6(16)
C8	42(2)	36(2)	27.3(19)	-0.5(16)	-2.6(17)	1.4(17)
C14	29.6(19)	39(2)	27.1(18)	0.0(16)	1.8(16)	5.0(16)
C10	35.3(19)	29.7(19)	27.9(18)	2.1(15)	-1.3(17)	1.0(16)
C7	49(2)	48(2)	31(2)	-5.9(18)	-7.4(19)	-4(2)
C2	42(2)	41(2)	38(2)	-3.2(18)	-3.7(19)	-6.7(18)
C12	35(2)	37(2)	26.0(18)	0.4(16)	0.9(17)	2.8(17)
C4	49(2)	40(2)	30.1(19)	2.5(17)	5.4(18)	-4.9(19)
C11	35(2)	35(2)	25.5(18)	-1.0(16)	0.3(16)	4.7(18)
C13	29.9(19)	42(2)	27.1(19)	-2.0(16)	0.7(16)	1.7(17)
C5	41(2)	44(2)	36(2)	2.1(19)	2.7(19)	-7.7(19)

C3	52(2)	45(2)	30(2)	-4.3(17)	-2.5(19)	-8(2)
C6	40(2)	46(2)	44(2)	1(2)	-2(2)	-9(2)

Table S3 Hydrogen atom coordinates ($Å \times 10^4$) and isotropic displacement parameters ($Å^2 \times 10^3$) for 8-hydroxyquinolinium hydrogen squarate.

Atom	***x***	***y***	***z***	**U(eq)**
H4A	-15790.42	-12971.45	-734.7	71
H1	-6403.63	-8621.98	-1129.15	41
H1A	-4163.21	-6669.6	-99.47	79
H7	-749.82	-5350.64	-449.74	52
H2	-7656.13	-9609.75	-1956.77	48
H4	-2231.67	-7506.31	-2762.04	48
H5	561.03	-5819.47	-2160.71	48
H3	-5588.44	-9016.51	-2808.15	51
H6	1458.29	-4765.9	-1272.69	52

Table S4 Values of torsion angles (°) for the 8-hydroxyquinolinium hydrogen squarate.

A-B-C-D	**Torsion Angle/°**
Hydrogen Squarate mono-anion	
C12-C11-C14-C13	-2.48(9)
C11-C14-C13-C12	2.33(6)
C14-C13-C12-C11	-2.29(9)
C13-C12-C11-C14	2.22(5)
O3-C12-C11-C14	-178.38(4)
O3-C12-C11-O2	4.44(10)
O3-C12-C13-C14	178.32(7)
O3-C12-C13-O4	-1.27(5)
O2-C11-C14-C13	174..86(2)
O2-C11-C14-O5	-4.76(2)
O2-C11-C12-C13	-174.95(11)
O5-C14-C13-C12	-178.02(5)

O5-C14-C13-O4	1.54(4)
O5-C14-C11-C12	178.12(8)
O4-C13-C12-C11	178.11(8)
O4-C13-C14-C11	-178.11(5)
8-Hydroxyquinolinium cation	
N1-C9-C8-O1	1.52(4)
N1-C9-C10-C4	1.18(2)
N1-C9-C10-C5	179.18(16)
N1-C2-C3-C4	1.33(3)
C2-C3-C4-C10	-1.99(11)
C2-N1-C9-C10	-1.91(10)
C3-C4-C10-C5	-177.16(7)
C4-C10-C5-C6	177.04(16)
C10-C5-C6-C7	0.78(18)
C10-C9-C8-O1	-179.73(6)
C5-C6-C7-C8	-0.28(5)
C5-C10-C9-C8	0.41(7)
C6-C7-C8-O1	179.64(19)
C6-C7-C8-C9	-0.16(9)
C7-C8-C9-N1	-178.66(3)
C7-C8-C9-C10	0.09(2)
C8-C9-N1-C2	176.87(17)

S4. Fingerprint analysis

The 2-D fingerprint plot of d_e versus d_i epitomizes all the intermolecular interactions in the crystal system (Spackman & McKinnon, 2002). The overall 2-D fingerprint plots for the two moieties and those decomposed into O···H/H···O, C···H/H···C, H···H, C···O/O···C, C···C, C···N/N···C, N···H/H···N, N···O/O···N and O···O interactions are displayed in Fig. S3 and S4. The relative percentages from various intermolecular interactions to the Hirshfeld surfaces of hydrogen squarate mono-anion and 8-hydroxyquinolinium cation are represented in a bar chart given in Fig. 9 in main manuscript.

For both moieties, the O···H/H···O contacts have the most significant contribution (36.3 % in 8-hydroxyquinolinium and 58.8 % in hydrogen squarate) to the total Hirshfeld surface. The sharp spike in the 2-D fingerprint plot represents H···O interaction (see Fig. S3(*b*)), which is due to large

proportion of hydrogen atoms present in the 8-hydroxyquinolinium cation. Due to higher proportion of oxygen atoms in the structure of squarate moiety there occurs a large spike in the bottom right area representing O···H interaction (see Fig. S4(*b*)). The O···H/H···O interaction is due to the presence of O-H···O, N-H···O and C-H···O short inter-atomic hydrogen bonds (see Table 4 in main manuscript). The bottom right area (see Fig. S3(*c*)) shows C···H (14.4 %) interactions and top left area represents H···C (11.1 %) interactions for 8-hydroxyquinolinium moiety. These significant contributions (25.5 %) from C···H/H···C contacts to the Hirshfeld surface indicate the presence of influential C-H···π interactions in the cation. However, for squarate moiety (see Fig. S4(*c*)) there is comparatively less contribution from C···H/H···C contacts (10.2 %) to the Hirshfeld surface.

The contribution of H···H contacts to the Hirshfeld surface of cation (24.6 %; Fig. S3(*d*)) and anion (3.4 % Fig. S4(*d*)) clearly explains the hydrogen richness and deficiency in cation and anion, respectively. Fig. S4(*e*) shows the fin-like distribution for C···O/O···C interactions with a 13.5 % contribution to the Hirshfeld surface and tips appearing at $d_i + d_e \sim 3.1$ Å for anion. However, for cation (Fig. S3(*e*)) there is comparatively less contribution from C···O/O···C interactions (6.7 %) to the molecular surface. The fingerprint plots delineated into C···C contacts show that these contacts have nearly the same contributions to the overall Hirshfeld surfaces of cation (3.2 %; Fig. S3(*f*)) and anion (3.5 %; Fig. S4(*f*)). The C···C contacts indicate the presence of π-π stacking in the crystal packing. The electronic and optical properties of the material are strongly correlated with the directionality of π-π and O···H interactions, which contributes to anisotropic properties of the single crystal.

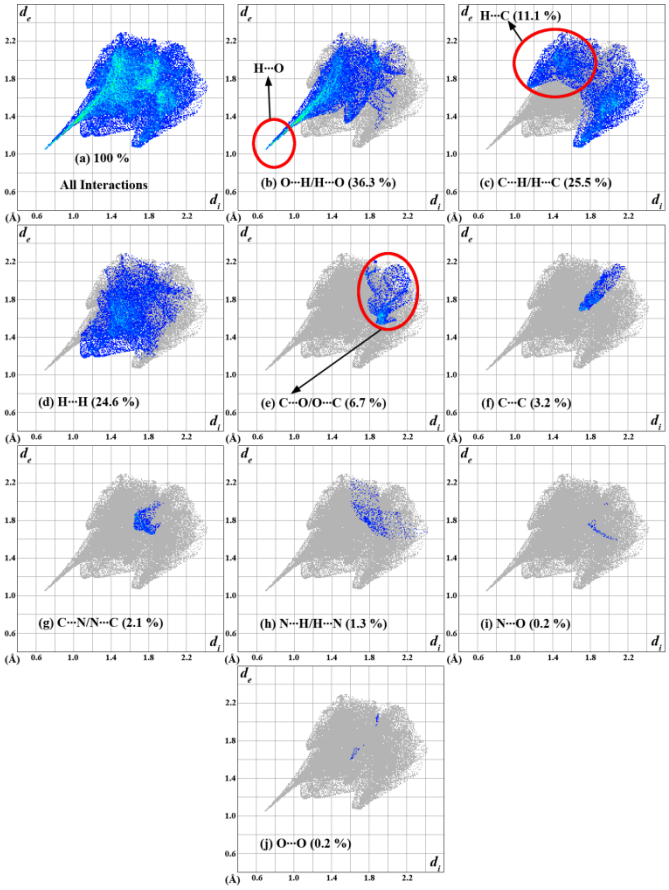

Figure S3 2-D fingerprint plots exemplifying contributions of various molecular interactions for 8-hydroxyquinolinium moiety.

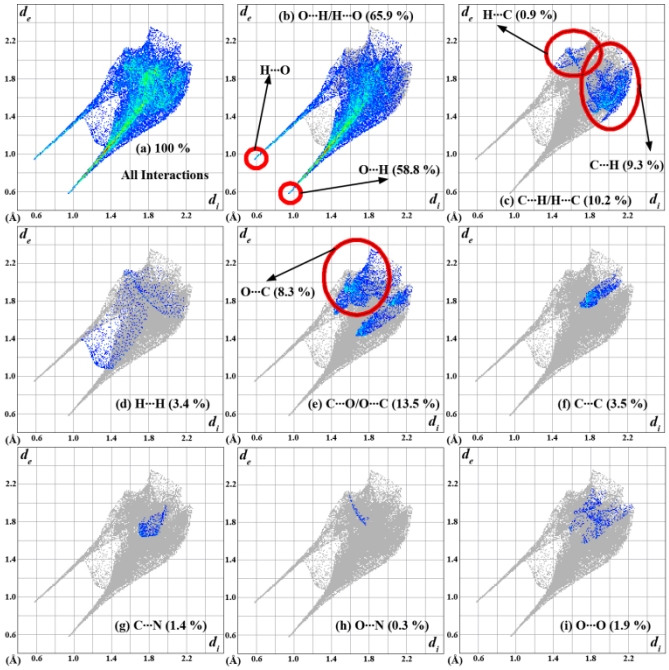

Figure S4 2-D fingerprint plots exemplifying contributions of various molecular interactions for hydrogen squarate mono-anion.

In both cation and anion, the interatomic C···N/N···C, N···H/H···N, N···O/O···N and O···O contacts contributes very little to the overall Hirshfeld surfaces. In spite of their smaller contributions, these interactions play a very significant role in crystal packing.

S5. Shape index, curvedness and void mapping

The shape index and curvedness (*C*) map are the two effective tools employed to study the local shape efficiency and measure the surface curvature of 3-D surfaces (McKinnon *et al.*, 2004). Fig. S5(*a*) and S5(*b*) illustrate the front and rear side of Hirshfeld surface of HQS molecule with shape index and curvedness mapped onto the surface, respectively. Hirshfeld surface with shape index mapped onto the surface can be used to visualize the regions where two molecular surfaces touch one another. Blue and red regions represent complementary bumps and hollow regions, respectively. The bright red hollow sites marked with arrows 1, 2 and 3 in Fig. S5(*a*) indicate the C···O, O···H and H···C interactions, respectively. Maps of *C* are used to recognize the planer and curved regions in HQS molecule. From Fig. S5(*b*), we see that large segments of flat green region are separated by blue color edges in the molecular surface.

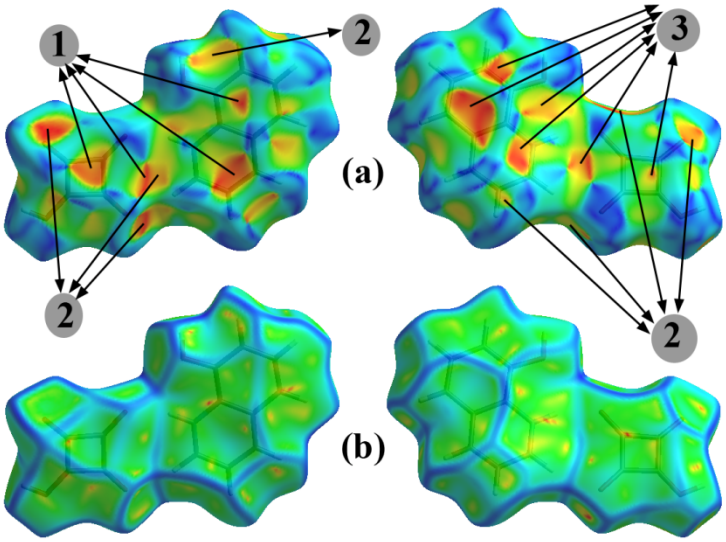

Figure S5 The front and rear side of molecular Hirshfeld surface of the HQS molecule mapped over (*a*) shape index and (*b*) curvedness.

The void mapping was performed using the isosurface of procrystal electron density at 0.002 au contour (Turner *et al.*, 2011). Fig. S6 shows the unit cell packing diagram along with voids of the HQS compound along '*c*' crystallographic axis. The uniformly distributed void channels were found to occupy 6.02 % of the unit cell volume with surface area of 334.87 Å^2. From the simulation of cavities present in the HQS crystal, we can infer that the void regions are uniformly distributed in its unit cell, which contributes further scope of bonding of titled molecule with metal ions to alter its anisotropic properties.

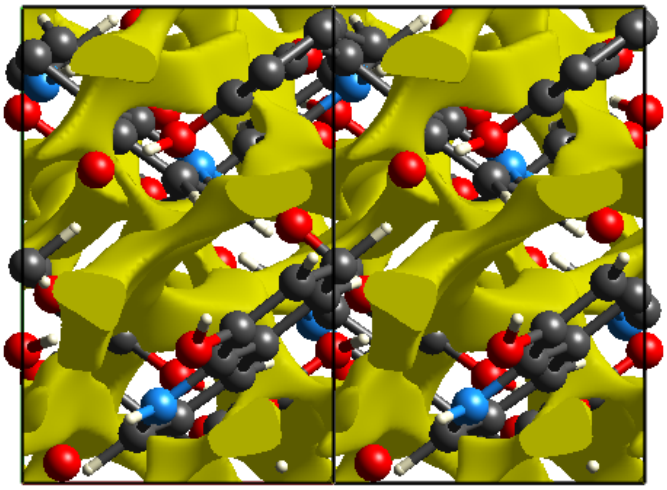

Figure S6 Unit cell packing diagram for HQS crystal with 0.002 au void surface. The view is along the '*c*' crystallographic axis.

References

McKinnon, J. J., Spackman, M. A. & Mitchell, A. S. (2004). *Acta Crystallogr. Sect. B Struct. Sci.* **60**, 627–668.

Rohlíček, J., Skořepová, E., Babor, M. & Čejka, J. (2016). *J. Appl. Crystallogr.* **49**, 2172–2183.

Spackman, M. A. & McKinnon, J. J. (2002). *CrystEngComm*. **4**, 378–392.

Turner, M. J., McKinnon, J. J., Jayatilaka, D. & Spackman, M. a. (2011). *CrystEngComm*. **13**, 1804–1813.